Jul 13th, 3:10 PM - 3:30 PM

A mathematical model for GHG from SB-MBR: calibration by an innovative protocol

Giorgio Mannina
Universita di Palermo, giorgio.mannina@unipa.it

Alida Cosenza
Universita di Palermo, alida.cosenza@unipa.it

International Environmental Modelling and Software Society (iEMSs)
8th International Congress on Environmental Modelling and Software
Toulouse, France, Sabine Sauvage, José-Miguel Sánchez-Pérez, Andrea Rizzoli (Eds.)
http://www.iemss.org/society/index.php/iemss-2016-proceedings

A mathematical model for GHG from SB-MBR: calibration by an innovative protocol

Mannina Giorgio[a], Alida Cosenza[a]
[a]*Dipartimento di Ingegneria Civile, Ambientale, Aerospaziale, dei Materiali, Università di Palermo, Viale delle Scienze, Ed.8, 90100, Palermo, Italy (e-mail:giorgio.mannina@unipa.it; alida.cosenza@unipa.it)*

Abstract: A mathematical model to quantify greenhouse gases (GHG) (carbon dioxide, CO_2 and nitrous oxide, N_2O) for a membrane bioreactor (MBR) is presented. The model has been applied to a pilot plant with a pre-denitrification MBR scheme. The pilot plant was cyclically filled with real saline wastewater according to the fill-draw-batch operation. The model was calibrated by adopting a specific protocol based on extensive field dataset. Standardised Regression Coefficient (SRC) method was adopted to select the most influential model factors to be calibrated. Results related to SRC method show that among the important model factors a key role is played by the half saturation coefficients related with the nitrogen removal processes (k_{N2O}, k_{NO}) and by the model factors affecting the oxygen transfer rate in the aerobic and MBR tank ($k_{2,2}$ and $k_{2,3}$). In terms of uncertainty, it was found that for the gaseous model outputs ($S_{GHG,N2O,1}$ and $S_{GHG,N2O,2}$) only the 7% and the 12% of the measured data lays outside the bands showing an accurate model prediction in case a wide data set is available.

Keywords*:* Uncertainty; greenhouse gases; wastewater; membrane.

1 INTRODUCTION

Greenhouse gases (CO_2, N_2O and CH_4) can be directly and indirectly produced by wastewater treatment plants (WWTPs). Direct emissions are mainly debited to the biological processes (emissions of CO_2 from microbial respiration, N_2O from nitrification and denitrification, and CH_4 from anaerobic digestion). Indirect emissions are mainly associated with the energy consumption. Among the GHGs produced by WWTPs, N_2O is the most environmentally hazardous due to its strong global warming potential (GWP) (298 higher that CO_2) and its capacity to deplete the stratospheric ozone layer (IPCC, 2013). N_2O can be produced both during nitrification and denitrification. During nitrification, ammonia oxidizing bacteria (AOB) have been recognized as the main contributor of N_2O production (Kampschreur et al., 2007; Yu et al., 2010). Two different pathways are involved during N_2O production by AOB: (i) the reduction of nitrite (NO_2^-) to N_2O via nitric oxide (NO) (AOB denitrification) (Chandran et al., 2011) and (ii) N_2O as a product of the incomplete oxidation of hydroxylamine (NH_2OH) to NO_2^-(Chandran et al., 2011). Several studies have demonstrated that the N_2O production is strongly depending on the plant operating conditions and on the influent wastewater features (Kampschreur et al., 2009; Peng et al., 2015). Therefore, a huge variations of N_2O emissions can be obtained among different WWTPs and inside the same plant due to the different features of the influent wastewater over the day (dynamic conditions). Despite such a statement, the United Nation's Intergovernmental Panel on Climate Change (IPCC) proposes to adopt simple model, often based on simple emission factor, to estimate the amount of N_2O produced by a WWTP. In this way the variability of the N_2O production due to the dynamic operational conditions is completely neglected (Corominas et al., 2012). In order to overcome such a substantial contradiction between the real conditions affecting the N_2O production in a WWTP and the suggestion to estimate their production, over the last years huge efforts have been performed by the scientific community in order to better quantify N_2O (Ni and Yuan, 2015). Several mathematical models have been proposed, tested and compared in literature in order to establish a reliable model (Corominas et al., 2012; Ni et al., 2013; Spérandio et al., 2016). Corominas et al. (2012) demonstrated that the assessment of GHGs by empirical models (based on a single emission factor) can produce erroneous results as the formation of GHGs is not a

linear process. Therefore, mechanistic process-based dynamic models are required to obtain an accurate estimation of GHG emissions. Ni et al. (2013) have compared four mathematical models able to separately describe the N_2O production by means of AOB as the final product of nitrifier denitrification or as a product of incomplete oxidation of hydroxylamine (NH_2OH). By adopting short-term batch experimental data Ni et al. (2013) found that none of the tested models was able to reproduce data. Moreover, the short term data should also be available for a good model calibration/validation (Ni et al., 2013). Very recently, Spérandio et al. (2016) adopted five activated sludge models describing N_2O production by AOB and compared the results to four different long-term process data sets. Differently to previous studies where only shot-term data gathered during batch tests were employed, Spérandio et al. (2016) adopted for the first time long term database to calibrate an N_2O models. Each model adopted by Spérandio et al. (2016) considers one of the two known N_2O production pathways by AOB (denitrification pathway and the hydroxylamine oxidation). Similarly, to Ni et al. (2013), Spérandio et al. (2016) found that, despite at least one of the investigated model was able to reproduce the measured data, none of the tested models describe all the N_2O data (obtained in the different systems) with a similar parameter set. To establish a reliable N_2O model, long term dataset and by a detailed knowledge on the parameters describing the microorganisms behaviour are thus needed (Sperandio et al., 2016). Very recently, with the aim to improve the N_2O quantification a new model combining two N_2O emission pathways by AOB was proposed and calibrated (adopting long-term data) by Pocquet et al. (2016) which showed good adaptation between measured and modelled data. Overall, literature shows, that maturity achieved in N_2O modelling has enabled the improvement of site-specific N_2O emissions (Ni and Yuan, 2015). However, despite the useful insights derived by N_2O mathematical models from WWTPs the derived results are likely to be subjected to a high degree of uncertainty (Sweetapple et al., 2013). Thus, the assessment of the uncertainty may improve the calibration process. With this aim the sensitivity and uncertainty analysis could help modeller to identify the key source affecting model outputs (Sweetapple et al., 2013). Despite the usefulness of uncertainty analysis only few studies have been performed in literature (Flores-Alsina et al., 2014; Sweetapple et al., 2013) mainly related to conventional activated sludge (CAS) system. Only recently, Mannina and Cosenza (2015) have presented a detailed uncertainty analysis of a new Activated Sludge Model (ASM2d) Soluble Microbial Product (SMP) – GHG model applied to a membrane bioreactor (MBR) University Cape Town (UCT) pilot plant. Mannina and Cosenza (2015) found that model factors related to the physical processes through the membrane could affect the GHG production. However, the study of Mannina and Cosenza (2015) have the limit of not being supported by GHG measured data.

In order to detail the GHG modelling in MBR plant, in this work a new mathematical model is presented. The mathematical model has been applied to a sequential batch (SB) MBR pilot plant fed with real saline wastewater. The model has been calibrated by adopting a detailed protocol developed in a previous study (Mannina et al., 2011b). A long-term data base (for dissolved and gaseous N_2O), acquired during an extensive gathering campaign, was adopted for the model calibration. Uncertainty analysis has also been performed.

2 MATERIAL AND METHODS

2.1 The mathematical model

The proposed model couples the ASM1 model (Henze et al., 2000) and the N_2O modelling production according to the approach of Hiatt and Grady (2008). The model has the peculiarity of including the SMPs modelling (formation/degradation of both utilisation associated products and biomass associated products) in order to take into account their influence on membrane fouling.

The mathematical model is divided into two sub-models: a biological sub-model and a physical sub-model. The physical sub-model simulates the main physical processes through the membrane: rate of sludge attachment and sludge detachment on the membrane surface during suction and backwashing phase, the solid mass deposition on the membrane surface, the thickness of the cake layer and the pore fouling by adopting the resistance in series model. The physical sub-model involves 6 model factors. For sake of conciseness for a detailed description of the physical sub-model the reader is referred to the literature (Mannina et al., 2011a). The biological sub-model involves: 16 biological processes (aerobic and anoxic); 19 state variables, which include dissolved N_2O and CO_2 (S_{N2O} and S_{CO2}, respectively) and 68 model factors. In the Appendices A and B, the Gujer Matrix and the process rate equations of the biological model are reported, respectively. The model also includes the stripping

processes for N_2O and CO_2 in order to evaluate the gaseous N_2O and CO_2 ($S_{GHG,N2O}$ and $S_{GHG,CO2}$). According to the Hiatt and Grady (2008) approach the nitrogen removal process is described as a two steps nitrification and four steps denitrification processes. With this regard the autotrophic biomass is modelled as ammonia-oxidising biomass (X_{AOB}) and nitrite oxidising biomass (X_{NOB}). In order to model the SMP formation/degradation the aerobic and anoxic hydrolysis processes related both to the UAP (S_{UAP}) and BAP (S_{BAP}) have been added in the ASM1 (see Appendix B). The rate of the anoxic hydrolysis of S_{BAP} is provided in Equation 1.

$$k_{h,BAP} \cdot \eta_{NO3,HYD} \cdot \left[\frac{K_{O2,HYD}}{K_{O2,HYD} + S_{O2}}\right] \cdot \left[\frac{S_{NO3}}{K_{NO3,HYD} + S_{NO3}}\right] \cdot S_{BAP} \cdot X_H \quad (1)$$

Further, the hydrolysis processes of X_s have also been added in the model.

Detailed description will be provided in the extension version of the manuscript. The biological model takes into account the influence of the salinity both for the autotrophic and heterotrophic biomass according to Park and Marchland (2006). More precisely, the maximum growth rate of both autotrophic and heterotrophic biomass has been reduced of the Is coefficient. This latter coefficient has been evaluated according to the Equation 2.

_____ (2)

Where I*s represent the inhibition factor evaluated and %NaCl is the percentage of salinity expressed as NaCl content.

2.2 The case study

An SB-MBR pilot plant consisted of two reactors in-series, one anoxic (volume 45 L) and one aerobic (volume 224 L), according to a pre-denitrification scheme (Figure 1) was monitored for three months. The pilot plant was equipped with an hollow fiber membrane module (Zenon Zeeweed, ZW10) installed into a separate aerated compartment (volume 50 L) for the solid liquid separation. An oxygen depletion reactor (ODR) was placed in the recycling line in order to ensure anoxic conditions inside the anoxic reactor despite the intensive aeration in the aerobic tank. The aerobic, anoxic and MBR reactors were equipped with specific covers that guaranteed the gas accumulation in the headspace.

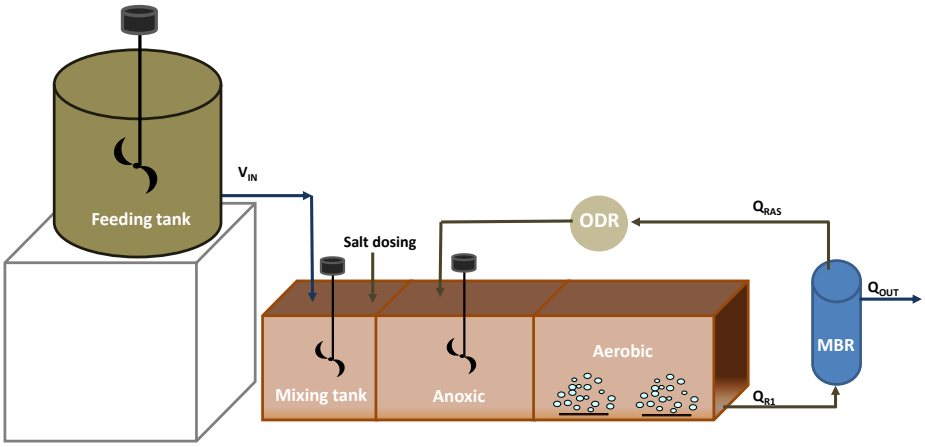

Figure 1. Layout of the SB-MBR pilot plant (where V_{IN} = 40 L = influent wastewater volume; ODR = Oxygen Depletion Reactor; MBR = membrane Bioreactor; Q_{RAS} = 80 L h^{-1} = recycled sludge from MBR to ODR; Q_{R1} = 80 L h^{-1} = sludge feeding from aerobic tank to MBR; Q_{OUT} = 20 L h^{-1} (only during the MBR filtration phase = effluent flow rate)

The SB-MBR pilot plant was discontinuously fed with real domestic wastewater (stored in a feeding tank of 320 L volume) according to fill-draw-batch operation approach. More in detail, 40 L of wastewater (V_{IN}) (previously mixed inside the mixing tank with salt, in order to meet the design salinity

concentration) were cyclically fed in, whereas the permeate was extracted at 20 L h^{-1} (Q_{OUT}). Each cycle had the duration of 3 hours that were split into 1 hour of biological reaction and 2 hours of MBR filtration. During the biological reaction time the permeate extraction pump was turned out, thus Q_{OUT} was equal to zero. During the cycle, 80 L h^{-1} (Q_{R1}) were continuously pumped from the aerobic to the MBR tank. Furthermore, a recycling activate sludge stream (Q_{RAS}), equal to 80 L h^{-1} during the reaction period and to 60 L h^{-1} (Q_{R1}-Q_{OUT}) during the filtration phase, was recycled from the MBR to the anoxic tank via the ODR tank. The experimental campaign was divided into six phases each characterized by a specific salt concentration from 0 up to 10 g NaCl L^{-1}. The NaCl concentration in the influent was increased at step of 2 g NaCl L^{-1} on a weekly basis. The Phase VI had a duration of 26 days. During the experimental campaign, gaseous and dissolved N_2O from the aerobic and anoxic tank were measured by using a Gas Chromatograph (Thermo Scientific™ TRACE GC) equipped with an Electron Capture Detector. Sample were withdrawn during an entire cycle (every 15 min for the gaseous sample and every 60 min for the liquid sample) at fixed salinity. During plant operations, the influent wastewater, the mixed liquor inside the anoxic and aerobic tank and the effluent permeate have been sampled and analyzed for total and volatile suspended solids (TSS and VSS), total chemical oxygen demand (COD_{TOT}), supernatant COD (COD_{SUP}), ammonium nitrogen (NH_4-N), nitrite nitrogen (NO_2-N), nitrate nitrogen (NO_3-N), total nitrogen (TN), phosphate (PO_4-P), total carbon (TC) and inert carbon (IC). Further details can be drawn from previous studies (Mannina et al., 2016b).

2.3 Calibration protocol and uncertainty estimation

Model calibration has been performed by adopting the calibration protocol as proposed by Mannina et al. (2011b). After a first trial and error calibration, the aforementioned protocol takes into account the selection of model factors of being calibrated for the model outputs of interest. Further, important model factors are calibrated on the basis of the measured data. More precisely the protocol takes into account the adoption of the generalized likelihood uncertainty estimation (GLUE) methodology (Beven and Binley, 1992); based on Monte Carlo simulations: a large number of model parameter sets are generated from the multidimensional parameter space, each with random parameter values selected from uniform probability distributions for each parameter in order to explore the whole confidence region. The acceptability of each set is assessed by comparing predicted to observed data throughout a chosen likelihood measure/efficiency. In this study the same likelihood measure as adopted by Mannina et al. (2011b) was used. The standardized regression coefficient (SRC) method has been adopted to select important model factors (1500 simulations were performed to adopt SRC) (Saltelli et al., 2004). The SRC method consists of a Monte Carlo simulation (with random sampling of the model factors) and a multivariate linear regression between the model output and the considered model factors. The absolute value of the standardised regression slopes of the regression (SRC or βi) represents the measure of sensitivity. The sign of βi indicates if the model factor "i" has positive (+) or negative (-) influence on the considered model output.
Regarding the uncertainty analysis, non important parameters are fixed to their default or trial and error calibration value. Further, only the model factors classified as important are considered to be uncertain and varied in the uncertainty range according to a random sampling.
The results of the Monte Carlo simulations were interpreted by evaluating the cumulative distribution function (CDF) for each model output. The 5^{th} and 95^{th} percentiles were also evaluated.

3 RESULTS AND DISCUSSION

For sake of conciseness in the following sections only the results related to the dissolved and gaseous N_2O (S_{N2O} and $S_{GHG,N2O}$) model output will be discussed. In detail, results relate to both anoxic (section 1) and aerobic (section 2) tank will be considered.

3.1 Sensitivity analysis

Figure 2 shows the results related to the important model factors at least for one of the model outputs considered: $S_{N2O,1}$ (a), $S_{GHG,N2O,1}$ (b), $S_{N2O,2}$ (c) and $S_{GHG,N2O,2}$ (d). For the meaning of the symbols reported in Figure 2 the reader is referred to the literature (Mannina and Cosenza, 2015). Among the important model factors, some merit to be discussed in detail. The group of half saturation coefficients (k_{N2O}, k_{NO3}, k_{ALK}) (related with the S_{N2O}, S_{NO3} and S_{ALK}) have a great influence on all the model outputs

considered. Such a result corroborates the literature findings, which indicate an high degree of uncertainty of the half-saturation coefficient related to the nitrogen transformation processes (Sweetapple et al., 2013). Therefore, when possible it is suggested to experimentally quantify these factors. The model factors $\mu_{AUT,AOB}$ and $\mu_{AUT,NOB}$ mostly affect (positively) the $S_{N2O,1}$ and $S_{GHG,N2O,2}$. Such a result shows an indirect effect for $S_{N2O,1}$. Indeed, with the increasing of the autotrophic maximum specific growth rate the availability of nitrate inside the aerobic tank increases with a consequent increase of $S_{N2O,1}$ produced during the denitrification for example due to the scares availability of substrate. The importance of the factors η_{g3} and η_{g4} for $S_{GHG,N2O,1}$ is of relevant interest. Indeed, these latter factors control the rate of the heterotrophic anoxic processes on the substrate (S_S) when S_{NO2} (nitrite) is reduced to S_{NO} (η_{g3}) and when S_{NO} (η_{g4}) is reduced into S_{N2O}. Thus, consequently influence the amount of gaseous N_2O emitted from the anoxic tank ($S_{GHG,N2O,1}$). The influence of $k_{2,2}$ and $k_{2,3}$ (coefficients for oxygen transfer of the aerobic tank and MBR tank, respectively) have both positive effect on $S_{N2O,1}$. Such a result is mainly debited to the fact that with the increasing of the oxygen concentration inside the aerobic and MBR tanks both the amount of nitrate and dissolved oxygen recycled into the anoxic tank increase. Therefore, the N_2O can be also produced due to the AOB contribution inside the anoxic tank (in case the environment become aerobic).

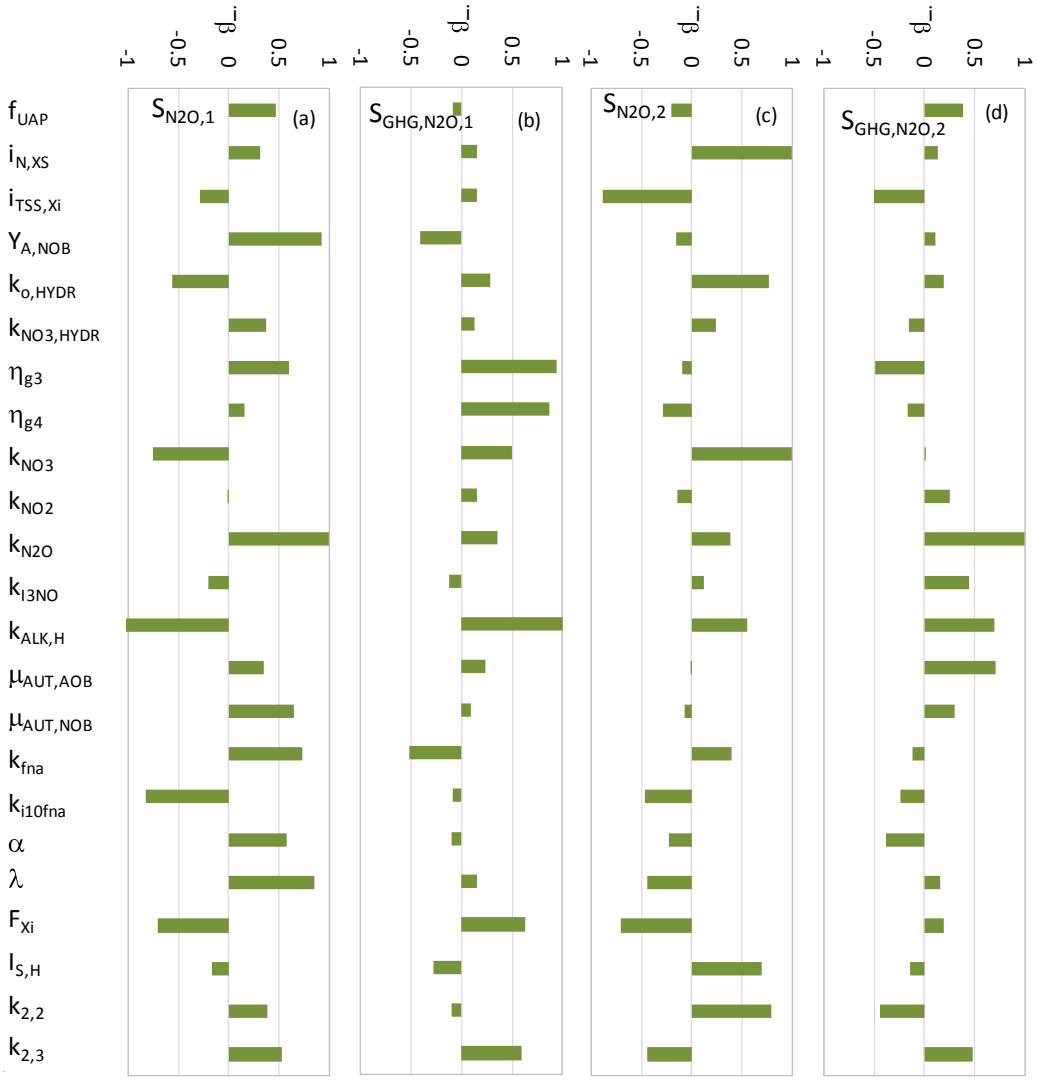

Figure 2. Results related to the SRC application for $S_{N2O,1}$ (a), $S_{GHG,N2O,1}$ (b), $S_{N2O,2}$ (c), $S_{GHG,N2O,2}$ (d) model outputs.

Thus, the role of $k_{2,2}$ and $k_{2,3}$ on $S_{N2O,1}$ is mainly indirect. Indeed, with the increase of $k_{2,3}$ the amount of the available oxygen inside the aerobic tank increases with a consequent complete nitrification. Therefore, the amount of nitrate to be denitrified in the anoxic tank increases; nitrate could not be completely denitrified due to the scarse availability of carbon. On the other hand, with the increase of

$k_{2,3}$ the amount of mass oxygen recycled from the MBR to the anoxic tank (through the ODR) increases. The importance of the factors affecting the oxygen transfer rate in the aerated tank suggests that in order to better predict N_2O emissions of a WWTP a detailed knowledge on the oxygen transfer has to be acquired.
Results of Figure 2, shows that the autotrophic salinity inhibition coefficient ($I_{s,H}$) positively influences the N_2O production inside the aerobic tank. Indeed, several studies have demonstrated that the salinity could promote the N_2O production during the nitrification (Zhao et al., 2014). It is interesting to note that factors related to the physical model (α and λ, representing the stickiness of the biomass particles and the screening parameter, respectively) affect both $S_{N2O,1}$ (Figure 2). Such a result is mainly debited to the role of the membrane in retaining the substrate that will be or not available for the nitrate denitrification.

3.3 Calibrated model

Table 1 summarizes the results related to the model efficiency. By analysing Table 1 one can observe that an acceptable adaption (the efficiency was almost always greater than 0.45; with exception of the model output related to the MBR tank) between measured an modelled data was obtained. The lower efficiency for the model output related to the MBR tank can be likely debited to the lower number of measured data with respect to the other sections.

Table 1. Synthesis of efficiency for each measured state variable

Section	Anoxic tank					
Model output	$COD_{TOT,1}$	$COD_{SUP,1}$	$X_{TSS,1}$	$S_{NO3,1}$	$S_{GHG,N2O,1}$	$S_{N2O,1}$
Efficiency	0.42	0.52	0.31	0.44	0.47	0.34
n° data	14	14	16	17	65	15
Section	Aerobic tank					
Model output	$COD_{TOT,2}$	$COD_{SUP,2}$	$X_{TSS,2}$	$S_{GHG,N2O,2}$	$S_{N2O,2}$	
Efficiency	0.46	0.52	0.46	0.49	0.39	
n° data	14	14	14	65	15	
Section	MBR tank					
Model output	$COD_{TOT,3}$	$COD_{SUP,3}$	$S_{NH4,3}$	$S_{NO3,3}$		
Efficiency	0.25	0.29	0.31	0.28		
n° data	8	8	8	8		
Section	Permeate					
Model output	$COD_{TOT,4}$	$S_{NH4,4}$	$S_{NO3,4}$	$TN_{,4}$		
Efficiency	0.35	0.34	0.36	0.3		
n° data	15	17	17	12		

3.2 Uncertainty analysis

In Figure 3 the CDF of calibrated, measured, 5th and 95th percentiles for $S_{GHG,N2O,1}$ (a), $S_{N2O,1}$ (b), $S_{GHG,N2O,2}$ (c) and $S_{N2O,2}$ (d) are reported.
By analysing data reported in Figure 3 one can observe that the uncertainty band width (as average difference between 95% and 5% percentile) changes with the model outputs in the different plant sections (e.g., greater for $S_{GHG,N2O,1}$ and $S_{N2O,2}$). Such a result is mainly due to the fact that some model outputs entail different level of complexity in terms of involved phenomena in the different plant sections. Further, the variation of some factors could make more uncertain the N_2O production in a certain section due to the overlapping effects among different processes. For example the increase of $k_{2,2}$ and $k_{2,3}$ could make the environment aerobic in a certain time during the cycle inside the anoxic tank. Therefore, both aerobic and anoxic N_2O formation could occur inside the anoxic tank.
By analysing data of Figure 3 it is possible to observe that for the model outputs for which a greater number of measured data was available ($S_{GHG,N2O,1}$ and $S_{GHG,N2O,2}$) a more accurate prediction can be obtained by adopting model. Indeed, for $S_{GHG,N2O,1}$ and $S_{GHG,N2O,2}$ only the 7% and the 12% of the measured data lays outside the band width. Such a result is of paramount interest, suggesting that long extensive data base are required to set up accurate model and to reduce the model uncertainty associated with the model predictions. Indeed, the 60% and the 46 % of the measured data lays

outside the band width for $S_{N2O,1}$ and $S_{N2O,2}$, respectively. More precisely, the measured data lower than 0.01 mgN L^{-1} and 0.025 mgN L^{-1} lays outside the band for $S_{N2O,1}$ and $S_{N2O,2}$, respectively.

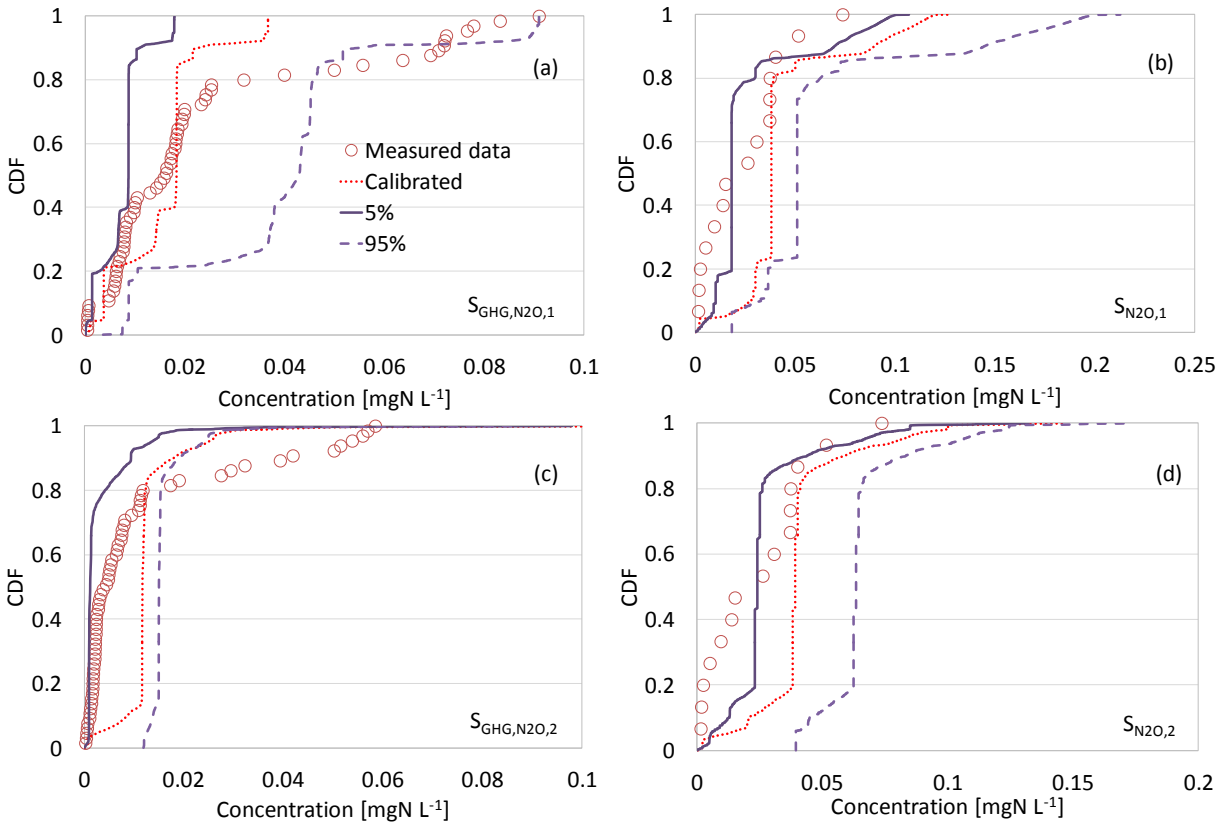

Figure 3. CDF related to the measured data, calibrated model, 5% and 95% percentiles for $S_{GHG,N2O,1}$ (a), $S_{N2O,1}$ (b), $S_{GHG,N2O,2}$ (c) and $S_{N2O,2}$ (d).

3 CONCLUSIONS

The main conclusions from this study can be drawn:

- ✓ An accurate knowledge on the model factors related to the oxygen transfer, in the aerated tanks, and on the half-saturation coefficients related to the nitrogen removal could improve the model predictions. Therefore, lab tests to acquire these data are suggested.
- ✓ Factors related to the membrane solid-liquid separation can indirectly affect N_2O production due to their capability to influence the higher or lower availability of the substrate during the denitrification.
- ✓ Model outputs for which a greater number of measured data was available ($S_{GHG,N2O,1}$ and $S_{GHG,N2O,2}$) a more accurate model prediction occurred, thus suggesting that a long term extensive database has to be required for the setting up of an accurate model to predict N_2O.

ACKNOWLEDGMENTS

This project was supported by the Italian Ministry of Education, University and Research (MIUR) through the Research project PRIN2012 (D.M. 28/12/2012 n. 957/Ric – Prot. 2012PTZAMC - http://ghgfromwwtp.unipa.it) in which the first author is the Principal Investigator.

REFERENCES

Beven, K.J., Binley, A., 1992 The future of distributed models: model calibration and uncertainty prediction. Hydrol. Proc. 6(3), 279–298.

Chandran, K., Stein, L.Y., Klotz, M.G., van Loosdrecht, M.C.M., 2011. Nitrous oxide production by lithotrophic ammonia-oxidizing bacteria and implications for engineered nitrogen-removal systems. Biochem. Soc. Trans. 39, 1832–1837.

Corominas, L., Flores-Alsina, X., Snip, L., Vanrolleghem, P.A., 2012. Comparison of different modeling approaches to better evaluate greenhouse gas emissions from whole wastewater treatment plants. Biotechnol. Bioeng. 109, 2854–2863.

Cosenza, A., Mannina, G., Vanrolleghem, P.A., Neumann, M.B., 2013. Global sensitivity analysis in wastewater applications: A comprehensive comparison of different methods Environmental Modelling & Software 49, 40-52.

Henze, M., Gujer, W., Mino, T. & Van Loosdrecht, M. 2000 Activated sludge models ASM1, ASM2, ASM2d and ASM3. In: IWA Task Group on Mathematical Modelling for Design and Operation of Biological Wastewater Treatment. IWA Publishing, London, UK.

Hiatt, W.C., Grady Jr, C.P.L., 2008. An updated process model for carbon oxidation, nitrification, and denitrification, Water Environ. Res. 80, 2145–2156.

IPCC, Climate Change, 2013. The Physical Science Basis. Contribution of Working Group I to the Fifth Assessment Report of the Intergovernmental Panel on Climate Change. 2013. Cambridge University Press, Cambridge, United Kingdom and New York, NY, USA, p. 1535.

Kampschreur, M.J., Tan, N.C.G., Kleerebezem, R., Picioreanu, C., Jetten, M.S.M., Loosdrecht, M.C.M., 2007. Effect of dynamic process conditions on nitrogen oxides emission from a nitrifying culture. Environ. Sci. Technol. 42, 429–435.

Kampschreur, M.J., Temmink, H., Kleerebezem, R., Jetten, M.S.M., Van Loosdrecht, M., 2009. Nitrous oxide emission during wastewater treatment. Water Res. 43, 4093–4103.

Mannina, G. Di Bella, G., Viviani, G., 2011a. An integrated model for biological and physical process simulation in membrane bioreactors (MBR). J. Membr. Sci. 376(1–2), 56–69.

Mannina, G., Cosenza, A., Vanrolleghem, P.A., Viviani, G., 2011b. A practical protocol for calibration of nutrient removal wastewater treatment models. Journal of Hydroinformatics 13.4, 575-595.

Mannina, G., Cosenza, A., 2015. Quantifying sensitivity and uncertainty analysis of a new mathematical model for the evaluation of greenhouse gas emissions from membrane bioreactors. Journal of Membrane Science 475, 80–90.

Mannina, G., Ekama, G., Caniani, D., Cosenza, A., Esposito, G., Gori, R., Garrido-Baserba, M., Rosso, D., Olsson, G., 2016a. Greenhouse gases from wastewater treatment — A review of modelling tools. Science of the Total Environment 551–552, 254–270.

Mannina G., Capodici M., Cosenza A., Di Trapani D., Viviani G. 2016b. Sequential Batch Membrane BioReactor for wastewater treatment: effect of salinity increase. Bioresour. Technol. 209, 205-212.

Ni, B.-J., Yuan, Z., 2015. Recent advances in mathematical modeling of nitrous oxides emissions from wastewater treatment processes. Water Research 87, 336–346.

Ni, B.-J., Yuan, Z., Chandran, K., Vanrolleghem, P.A., Murthy, S., 2013. Evaluating four mathematical models for nitrous oxide production by autotrophic ammonia oxidizing bacteria. Biotechnol. Bioeng. 110, 153–163.

Park C., Marchland E.A., 2006. Modelling Salinity Inhibition Effects During Biodegradation of Perchlorate. J. Appl. Microbiol., 101, 222-233.

Peng, L., Ni, B.-J., Ye, L., Yuan, Z., 2015. The combined effect of dissolved oxygen and nitrite on N2O production by ammonia oxidizing bacteria in an enriched nitrifying sludge. Water Res. 73C, 29–36.

Pocquet, M, Wu, Z., Queinnec, I., Spérandio, M., 2016. A two pathway model for N_2O emissions by ammonium oxidizing bacteria supported by the NO/N_2O variation. Water Res. 88, 948-959.

Saltelli, A. Tarantola, S. Campolongo, F. Ratto, M. Sensitivity analysis in practice. A guide to assessing scientific models, Probability and Statistics Series, John Wiley & Sons Publishers, Chichester, England, 2004.

Spérandio, M., Pocquet, M., Guo, L., Ni, B.-J., Vanrolleghem, P.A., Yuan, Z., 2016. Evaluation of different nitrous oxide production models with four continuous long-term wastewater treatment process data series. Bioprocess Biosyst Eng. 39(3), 493-510.

Sweetapple, C., Fu, G., Butler, D., 2013. Identifying key sources of uncertainty in the modelling of greenhouse gas emissions from wastewater treatment, Water Res.47, 4652–4665.

Yu, R., Kampschreur, M.J., Loosdrecht, M.C.M., Chandran, K., 2010. Mechanisms and specific directionality of autotrophic nitrous oxide and nitric oxide generation during transient anoxia. Environ. Sci. Technol. 44, 1313–1319.

Zhao, W., Wang, Y., Lin, X., Zhou, D., Pan, M., Yang, J., 2014. Identification of the salinity effect on N_2O production pathway during nitrification: Using stepwise inhibition and 15N isotope labeling methods. Chem. Eng. J. 253 418–426.

Appendix A: Gujer Matrix of the SB-MBR biological sub-model; ; in grey the new hydrolysis processes added with respect to ASM1

Process	S_{O2}	S_S	S_{BAP}	S_{UAP}	S_{NH4}	S_{NO3}	S_{NO2}	S_{NO}	S_{N2O}	S_{N2}	S_I	S_{ALK}	S_{CO2}	X_I	X_S	X_H	X_{AOB}	X_{NOB}	X_{TSS}
1		1-f_{SI}	-1								f_{SI}								
2		1-f_{SI}	-1								f_{SI}								
3		1-f_{SI}		-1							f_{SI}								
4		1-f_{SI}		-1							f_{SI}								
5		1-f_{SI}			$\nu_{5,5}$						f_{SI}	i_{Charge_NH4}*$\nu_{5,5}$			-1				-$i_{TSS,XS}$
6		1-f_{SI}			$\nu_{5,6}$						f_{SI}	i_{Charge_NH4}*$\nu_{5,6}$			-1				-$i_{TSS,XS}$
7	$\nu_{1,7}$	$-\frac{1}{Y_H}$		$\frac{f_{UAP}}{Y_H}$	$\nu_{5,7}$							i_{Charge_NH4}*$\nu_{5,7}$	$\nu_{13,7}$			1			$i_{TSS,BM}$
8		$\nu_{2,8}$		$\nu_{4,8}$	$\nu_{5,8}$	$\nu_{6,8}$	$\nu_{7,8}$					i_{Charge_NH4}*$\nu_{5,8}$+i_{Charge_NO3}*$\nu_{6,8}$+i_{Charge_NO2}*$\nu_{7,8}$	$\nu_{13,8}$			1			$i_{TSS,BM}$
9		$\nu_{2,9}$		$\nu_{4,9}$	$\nu_{5,9}$		$\nu_{7,9}$	$\nu_{8,9}$				i_{Charge_NH4}*$\nu_{5,9}$+ i_{Charge_NO2}*$\nu_{7,9}$	$\nu_{13,9}$			1			$i_{TSS,BM}$
10		$\nu_{2,10}$		$\nu_{4,10}$	$\nu_{5,10}$			$\nu_{8,10}$	$\nu_{9,10}$			i_{Charge_NH4}*$\nu_{5,10}$	$\nu_{13,10}$			1			$i_{TSS,BM}$
11		$\nu_{2,11}$		$\nu_{4,11}$	$\nu_{5,11}$				$\nu_{9,11}$	$\nu_{10,11}$		i_{Charge_NH4}*$\nu_{5,11}$	$\nu_{13,11}$			1			$i_{TSS,BM}$
12			f_{BAP}		$\nu_{5,12}$							i_{Charge_NH4}*$\nu_{5,12}$	$\nu_{13,12}$	f_{XI}	1-f_{XI}-f_{BAP}	-1		f_{XI}*$i_{TSS,BM}$+(1-f_{XI})*$i_{TSS,XS}$-$i_{TSS,BM}$	
13	$\nu_{1,13}$			$\frac{f_{UAP}}{Y_{AOB}}$	$-i_{N,BM}-\frac{f_{UAP}}{Y_{AOB}}$	$\frac{1}{Y_{AOB}}$	$-\frac{1}{Y_{AOB}}$					$\nu_{5,13}$*i_{Charge_NH4}+ $\frac{1}{Y_{AOB}}$ i_{Charge_NO2}	$\nu_{13,13}$				1			$i_{TSS,BM}$
14	$\nu_{1,14}$				-$i_{N,BM}$							$\nu_{5,14}$*i_{Charge_NH4}+ $\frac{1}{Y_{NOB}}$ i_{Charge_NO3} $-\frac{1}{Y_{NOB}}$ *i_{Charge_NO2}	$\nu_{13,14}$					1	$i_{TSS,BM}$
15			f_{BAP}		$\nu_{5,15}$							i_{Charge_NH4}*$\nu_{5,15}$	$\nu_{13,15}$	f_{XI}	1-f_{XI}-f_{BAP}		-1		f_{XI}*$i_{TSS,XI}$+(1-f_{XI})*$i_{TSS,XS}$-$i_{TSS,BM}$
16			f_{BAP}		$\nu_{5,16}$							i_{Charge_NH4}*$\nu_{5,16}$	$\nu_{13,16}$	f_{XI}	1-f_{XI}-f_{BAP}			-1	f_{XI}*$i_{TSS,XI}$+(1-f_{XI})*$i_{TSS,XS}$-$i_{TSS,BM}$

$$\upsilon_{5,5-6}=-\left(-f_{SI}\right)\cdot i_{N,S_S}+f_{SI}\cdot i_{N,SI}-i_{N,XS};\ \upsilon_{1,7}=-\frac{-Y_H-f_{UAP}}{Y_H};\upsilon_{1,13}=-\frac{\left(-\frac{16}{14}-i_{COD\_NO3}-Y_{AOB}-f_{UAP}\right)}{Y_{AOB}};\upsilon_{1,14}=-\frac{\left(COD\_NO2-i_{COD\_NO3}-Y_{NOB}-f_{UAP}\right)}{Y_{NOB}};\upsilon_{2,8-12}=-\frac{1}{Y_H\eta_{Y\_H}};\upsilon_{4,8-11}=\frac{f_{UAP}}{Y_H\eta_{Y\_H}};\upsilon_{5,7}=-i_{N,BM};\upsilon_{5,18-11}=-i_{N,BM};\upsilon_{5,12}=\upsilon_{5,15-16}=-\left(i_{XI}\cdot i_{N,XI}+\left(-f_{XI}\right)\cdot i_{N,XS}-i_{N,BM}\right)$$

$$\upsilon_{6,8}=\frac{\left(-\left(Y_H\cdot\eta_{Y\_H}\right)-f_{UAP}\right)}{\left(COD\_NO3-i_{COD\_NO2}\right)Y_H\cdot\eta_{Y\_H}};\upsilon_{7,8}=-\frac{1-\left(Y_H\cdot\eta_{Y\_H}\right)}{\left(COD\_NO3-i_{COD\_NO2}\right)Y_H\cdot\eta_{Y\_H}}\ \upsilon_{7,9}=-\upsilon_{8,9}=\upsilon_{8,10}=\frac{1-\left(Y_H\cdot\eta_{Y\_H}\right)-f_{UAP}}{\left(COD\_NO2-i_{COD\_NO}\right)Y_H\cdot\eta_{Y\_H}};\upsilon_{9,11}=\frac{1-\left(Y_H\cdot\eta_{Y\_H}\right)-f_{UAP}}{\left(COD\_N2O-i_{COD\_N2}\right)Y_H\cdot\eta_{Y\_H}};\upsilon_{10,11}=-\frac{1-\left(Y_H\cdot\eta_{Y\_H}\right)}{\left(COD\_N2O-i_{COD\_N2}\right)Y_H\cdot\eta_{Y\_H}}$$

Appendix B: Process rate equations of the biological sub-model; in grey the rate related to the new hydrolysis processes

No.	Process	Process rate equation ρ_j
1	Aerobic hydrolysis of BAP	$k_{h,BAP} \cdot \left[\frac{S_{O2}}{K_{O2,HYD}+S_{O2}}\right] \cdot S_{BAP} \cdot X_H$
2	Anoxic hydrolysis of BAP	$k_{h,BAP} \cdot \eta_{NO3,HYD} \cdot \left[\frac{K_{O2,HYD}}{K_{O2,HYD}+S_{O2}}\right] \cdot \left[\frac{S_{NO3}}{K_{NO3,HYD}+S_{NO3}}\right] \cdot S_{BAP} \cdot X_H$
3	Aerobic hydrolysis of UAP	$k_{h,UAP} \cdot \left[\frac{S_{O2}}{K_{O2,HYD}+S_{O2}}\right] \cdot S_{UAP} \cdot X_H$
4	Anoxic hydrolysis of UAP	$k_{h,UAP} \cdot \eta_{NO3,HYD} \cdot \left[\frac{K_{O2,HYD}}{K_{O2,HYD}+S_{O2}}\right] \cdot \left[\frac{S_{NO3}}{K_{NO3,HYD}+S_{NO3}}\right] \cdot S_{UAP} \cdot X_H$
5	Aerobic hydrolysis	$k_h \cdot \left[\frac{S_{O2}}{K_{O2,HYD}+S_{O2}}\right] \cdot \left[\frac{\frac{X_S}{X_H}}{K_X+\frac{X_S}{X_H}}\right] \cdot X_H$
6	Anoxic hydrolysis	$k_h \cdot \eta_{NO3,HYD} \cdot \left[\frac{K_{O2,HYD}}{K_{O2,HYD}+S_{O2}}\right] \cdot \left[\frac{S_{NO3}}{K_{NO3,HYD}+S_{NO3}}\right] \cdot \left[\frac{\frac{X_S}{X_H}}{K_X+\frac{X_S}{X_H}}\right] \cdot X_H$
7	Aerobic growth on S_S	$\mu_H \cdot \left[\frac{S_{O2}}{K_{O2,H}+S_{O2}}\right] \cdot \left[\frac{S_s}{K_s+S_S}\right] \cdot \left[\frac{S_{NH4}}{K_{NH4,H}+S_{NH4}}\right] \cdot \left[\frac{S_{ALK}}{K_{ALK}+S_{ALK}}\right] \cdot X_H$
8	Anoxic growth on S_S reducing NO_3 to NO_2	$\mu_H \cdot \eta_{g2} \cdot \left[\frac{K_{O2,H}}{K_{O2,H}+S_{O2}}\right] \cdot \left[\frac{S_{NO3}}{K_{NO3}+S_{NO3}}\right] \cdot \left[\frac{S_s}{K_s+S_s}\right] \cdot \left[\frac{S_{NH4}}{K_{NH4,H}+S_{NH4}}\right] \cdot \left[\frac{S_{ALK}}{K_{ALK}+S_{ALK}}\right] \cdot X_H$
9	Anoxic growth on S_S reducing NO_2 to NO	$\mu_H \cdot \eta_{g3} \cdot \left[\frac{K_{O2,H}}{K_{O2,H}+S_{O2}}\right] \cdot \left[\frac{S_{NO2}}{K_{NO2}+S_{NO2}}\right] \cdot \left[\frac{S_S}{K_S+S_s}\right] \cdot \left[\frac{S_{NH4}}{K_{NH4,H}+S_{NH4}}\right] \cdot \left[\frac{S_{ALK}}{K_{ALK}+S_{ALK}}\right] \cdot \left[\frac{K_{I3NO}}{K_{I3NO}+S_{NO}}\right] \cdot X_H$
10	Anoxic growth on S_S reducing NO to N_2O	$\mu_H \cdot \eta_{g4} \cdot \left[\frac{K_{O2,H}}{K_{O2,H}+S_{O2}}\right] \cdot \left[\frac{S_{NO}}{K_{NO}+S_{NO}+\frac{S^2{}_{NO}}{K_{I4NO}}}\right] \cdot \left[\frac{S_S}{K_S+S_S}\right] \cdot \left[\frac{S_{NH4}}{K_{NH4,H}+S_{NH4}}\right] \cdot \left[\frac{S_{ALK}}{K_{ALK}+S_{ALK}}\right] \cdot \left[\frac{K_{I3NO}}{K_{I3NO}+S_{NO}}\right] \cdot X_H$
11	Anoxic growth on S_S reducing N_2O to N_2	$\mu_H \cdot \eta_{g5} \cdot \left[\frac{K_{O2,H}}{K_{O2,H}+S_{O2}}\right] \cdot \left[\frac{S_{N2O}}{K_{N2O}+S_{N2O}}\right] \cdot \left[\frac{S_S}{K_S+S_S}\right] \cdot \left[\frac{S_{NH4}}{K_{NH4,H}+S_{NH4}}\right] \cdot \left[\frac{S_{ALK}}{K_{ALK}+S_{ALK}}\right] \cdot \left[\frac{K_{I5NO}}{K_{I5NO}+S_{NO}}\right] \cdot X_H$
12	Lysis of X_H	$b_H \cdot X_H$
13	Aerobic growth of X_{AOB}	$\mu_{AUT,AOB} \cdot \left[\frac{S_{O2}}{K_{O,AOB}+S_{O2}}\right] \cdot \left[\frac{S_{FA}}{K_{FA}+S_{FA}+\frac{S^2{}_{FA}}{K_{I9FA}}}\right] \cdot \left[\frac{K_{I9FNA}}{K_{I9FNA}+S_{FNA}}\right] \cdot \left[\frac{S_{ALK}}{K_{ALK,AUT}+S_{ALK}}\right] \cdot X_{AOB}$
14	Aerobic growth of X_{NOB}	$\mu_{AUT,NOB} \cdot \left[\frac{S_{O2}}{K_{O,NOB}+S_{O2}}\right] \cdot \left[\frac{S_{FNA}}{K_{FNA}+S_{FNA}+\frac{S^2{}_{FNA}}{K_{I10FNA}}}\right] \cdot \left[\frac{K_{I10FA}}{K_{I10FA}+S_{FA}}\right] \cdot \left[\frac{S_{ALK}}{K_{ALK,AUT}+S_{ALK}}\right] \cdot X_{NOB}$
15	Lysis X_{AOB}	$b_{AUT,AOB} \cdot X_{AOB}$
16	Lysis X_{NOB}	$b_{AUT,NOB} \cdot X_{NOB}$